

# Photolithographic Technique for Direct Photochemical Modification and Chemical Micropatterning of Surfaces

Kwangjoo Lee,<sup>†</sup> Feng Pan,<sup>‡</sup> Gregory T. Carroll,<sup>†</sup> Nicholas J. Turro,<sup>†,‡</sup> and Jeffrey T. Koberstein<sup>\*,‡</sup>

Department of Chemistry, 3000 Broadway, MC 3119, New York, New York 10027, and  
Department of Chemical Engineering, 500 West 120th Street, MC4721, Columbia University,  
New York, New York 10027

Received September 29, 2003. In Final Form: January 5, 2004

We describe a photolithographic method for the direct modification and micropatterning of the surface chemical structure of self-assembled monolayers. End-functional azobenzene alkanethiols are designed and synthesized so that, when self-assembled onto gold substrates, an acid-sensitive *tert*-butyl ester end group is positioned at the air–monolayer interface. Upon exposure to UV radiation in the presence of a photoacid generator, the *tert*-butyl ester groups are removed in the form of butylene gas to form surface carboxylic acid groups. The orientation of the monolayers and photochemical surface modification reactions are characterized by X-ray photoelectron spectroscopy measurements. The photochemical change from hydrophobic *tert*-butyl ester groups to hydrophilic carboxylic acid groups causes a significant change in wettability reflected in a water contact angle change from 89 to 28°, respectively. Surface chemical modifications may be patterned on a microscale by simply irradiating the self-assembled monolayers in the presence of a photoacid generator through a photomask. Chemically micropatterned surfaces are shown to be effective templates for patterned surface assembly of amine-terminated polystyrene colloidal particles and fluorescently tagged polystyrene nanoparticles and for the spatial patterning of water droplets. The photochemical changes that occur are constrained structurally to occur only at the air–monolayer surface and require only deep UV radiation and a photoacid generator as reagents. Direct photochemical micropatterning by this method is a simple and direct process that retains the full spatial resolution of deep UV photolithography and can be carried out with conventional photomasking equipment.

## Introduction

In many material applications, it is highly desirable to design and control the structure and properties of surfaces and interfaces without affecting the material's bulk properties. Exemplary surface properties of interest include wettability, adhesion, tack, friction and wear, hardness, and gloss. The task of modifying surfaces and interfaces to control such properties is a daunting one because many surface characteristics are related to the nature of chemical and physical structure on a molecular level. Few current techniques for surface modification, however, allow for specific chemical and structural control at molecular dimensions. In addition, many methods under development for surface modification are not readily suited to industrial application and scale-up. There exists, therefore, strong motivation to create molecular-based methods and processes that can be used to design and control the chemical and physical nature of surfaces and interfaces.

Ideally, surface modification strategies should involve few or no reagents, require only ambient conditions in a normal atmosphere, should be universal for a variety of substrate materials, and should not necessitate elaborate external processing operations. Most current surface modification strategies do not satisfy these conditions. Oxidative treatments<sup>1,2</sup> such as corona discharge, oxygen

plasma, or UV/ozone are rather indiscriminate and kinetic in nature, rendering the control of modification depth and surface chemistry difficult. These treatments are often unstable, with reorganization<sup>3,4</sup> of the surface usually taking place shortly after processing. Chemical treatment methods for surface modification<sup>1,2</sup> often require harsh and hazardous reagents, and the depth of modification can usually be confined to the surface only by regulating the exposure time.

A number of emerging material applications require molecular-level control of the spatial distribution of the chemical functionalities comprising the surface. Such patterned surfaces can be used as templates to create microarrays of biomolecules, including proteins<sup>5,6</sup> and DNA.<sup>7–9</sup> In addition, patterned surfaces can be used to precisely control the deposition of nanoparticles,<sup>10–12</sup> allowing for the design of three-dimensional architectures for use in next-generation electronic devices.

Several patterning technologies have been demonstrated, including nanografting,<sup>13</sup> microstamping,<sup>14,15</sup> and

\* To whom correspondence should be addressed. Tel.: (212) 854-3120. Fax: (212) 854-3054. E-mail: jk1191@columbia.edu.

<sup>†</sup> Department of Chemistry, Columbia University.

<sup>‡</sup> Department of Chemical Engineering, Columbia University.

(1) See, for example, Wu, S. *Polymer Interface and Adhesion*; Marcel Dekker: New York, 1982.

(2) See, for example, Garbassi, F.; Morra, M.; Occhiello, E. *Polymer Surfaces: from Physics to Technology*; Wiley: New York, 1998.

(3) Holly, F. J.; Refojo, M. F. Water Wettability of Hydrogels. *ACS Symp. Ser.* **1976**, 31, 252.

(4) Lewis, K. B.; Ratner, B. D. *J. Colloid Interface Sci.* **1993**, 159, 77.

(5) Blawas, A. S.; Reichert, W. M. *Biomaterials* **1998**, 19, 595.

(6) Bernard, A.; Delamarche, E.; Schmid, H.; Michel, B.; Bosshard, H. R.; Biebuyck, H. *Langmuir* **1998**, 14, 2225.

(7) Pirrung, M. C. *Angew. Chem., Int. Ed.* **2002**, 41, 1276.

(8) Gillmor, S. D.; Thiel, A. J.; Strother, T. C.; Smith, L. M.; Lagally, M. G. *Langmuir* **2000**, 16, 7223.

(9) Whitesides, G. M.; Ostuni, E.; Takayama, S.; Jiang, X.; Ingber, D. E. *Annu. Rev. Biomed. Eng.* **2001**, 3, 335.

(10) Alivisatos, A. P. *Endeavour* **1997**, 21, 56.

(11) Shipway, A. N.; Katz, E.; Willner, I. *ChemPhysChem* **2000**, 1, 18.

(12) Willner, I.; Willner, B. *Pure Appl. Chem.* **2002**, 74, 1773.

(13) Liu, G.; Xu, S.; Qian, Y. *Acc. Chem. Res.* **2000**, 33, 457.

(14) Kumar, A.; Abbott, N. L.; Biebuyck, H. A.; Kim, E.; Whitesides, G. M. *Acc. Chem. Res.* **1995**, 28, 219.

photolithography;<sup>16–21</sup> however, limitations are associated with each of these methods. Nanografting requires the use of atomic force and scanning tunneling microscopes and is a slow technique requiring physical contact with each spatial location in the pattern. Microstamping requires fabrication of both a positive and a negative mold and involves subsequent alignment of the stamps and a mechanical step to transfer physisorbed monolayers to the surface of the substrate. Photolithography involves the use of a patterned photomask containing opaque and translucent regions to choreograph regiospecific photochemical changes within a photoresist. The resolution of the patterned area is limited only by the wavelength of the light, but the technique suffers from the usual requirement of a development step to create the pattern.

In this report, we describe a new photolithographic technique for direct photochemical modification and patterning of surface properties of self-assembled monolayers (SAMs).<sup>22</sup> The specific technology employs a photoacid generator (PAG), a chemical species that releases a proton upon photolysis, to hydrolyze terminal *tert*-butyl ester groups located at the surface of a SAM to reactive carboxylic acid groups in a process that is almost devoid of reagents and safety hazards.<sup>23,24</sup> We demonstrate that the initially hydrophobic surface of the monolayer can be photochemically transformed into a hydrophilic surface with increased surface free energy and reactive binding sites for covalent attachment of nanoparticles and biomolecules. Regiospecific control of the surface free energy and surface functionality is achieved using only light, a PAG, and conventional photolithographic masking equipment. This work follows a medley of previous studies in which photochemical modifications have been used to create regular and spatially modulated changes in photoactive SAMs and ultrathin organic films. For example, PAGs have previously been used to induce hydrolysis of surface-grafted acid-sensitive polymers on a substrate surface, leading to changes in surface properties.<sup>25</sup> Irradiation of aromatic silane SAMs has been shown to produce silanols.<sup>26</sup> Likewise, photolysis of chloromethyl groups on phenyl siloxanes results in a phenyl aldehyde as the principle product.<sup>27</sup> Chemical techniques can then be coupled to these modifications to further alter surface reactivity. In conjunction with a photomask, SAMs containing photolabile groups provide a convenient method for building arrays of biomolecules.<sup>28,29</sup> Photochemical

attachment,<sup>30,31</sup> polymerization,<sup>32,33</sup> and oxidation<sup>34</sup> on surfaces have also been demonstrated. Our method expands the repertoire of photochemical modifications on surfaces, providing a route to transforming a *tert*-butyl group into a carboxylic acid, and demonstrates the use of a PAG to photochemically hydrolyze specified regions of a SAM.

## Experimental Section

**Synthesis of Azobenzene Derivatives. Compound 1, 4-[4-(6-Mercaptohexyloxy)phenylazo]benzoic Acid *tert*-Butyl Ester.** 4-[4-(6-Bromohexyloxy)phenylazo]benzoic acid *tert*-butyl ester was synthesized following a reported procedure.<sup>35,36</sup> 4-Aminobenzoic acid *tert*-butyl ester (Fluka, 4.81 g, 25 mmol) was stirred to dissolve in 55 mL of a dilute hydrochloric acid aqueous solution. After cooling in an ice bath, the acid mixture was diazotized by adding dropwise a solution of 1.73 g of NaNO<sub>2</sub> in 5 mL of water at 0 °C to the acid mixture in the ice water bath. The solution mixture turned a strong yellow. The solution was diluted with 100 mL of chilled methanol, and then coupling was carried out by adding the diazotized solution slowly to a chilled solution of phenol (2.34 g, 24 mmol), KOH (2.69 g, 48 mmol), and 25 mL of MeOH at 0 °C. An orange-yellow precipitate was formed. The solution was stirred for 2 h in an ice water bath. The precipitate was filtered off, dried, and recrystallized from *n*-hexane. An orange-yellow solid was obtained (6.41 g, 87%). A mixture of 3.4 mmol of 4-[4-(4-hydroxyphenylazo)]benzoic acid *tert*-butyl ester, 33.6 mmol of 1,6-dibromohexane, 16.8 mmol of dry potassium carbonate, and a catalytic amount of potassium iodide in 25 mL of dry acetone was stirred under reflux overnight. The completion of the reaction was confirmed by thin-layer chromatography analysis. After cooling, the precipitated salt was filtered off, and the filtrate was concentrated in vacuo. The crude product was purified by recrystallization from a hexane/ethyl acetate (70:30) mixture. A shiny orange powder (yield 91%, 1.41 g) was obtained.

4-[4-(6-Mercaptohexyloxy)phenylazo]benzoic acid *tert*-butyl ester was synthesized by applying the literature procedure for the synthesis of a similar molecule.<sup>37,38</sup> A total of 0.41 g (0.9 mmol) of prepared 4-[4-(6-bromohexyloxy)phenylazo]benzoic acid *tert*-butyl ester and 0.25 mg (1.1 mmol) of sodium thiosulfate pentahydrate in 5 mL of water was dissolved in 18 mL of ethanol and refluxed for 3 h. The mixture was then stirred at room temperature for another 1 h. After cooling, the precipitate was filtered off using a fritted funnel. A fine orange solid (bunte salt) was obtained. The salt was used without purification. Both 10 mL of chloroform and 10 mL of 1 M HCl were added to the bunte salt. The reaction mixture was refluxed for 2 h at 70 °C. The orange organic phase was extracted from the colorless aqueous layer. The collected organic layers were further extracted with 10 mL of chloroform (three times) and combined. The organic layers were washed with saturated NaHCO<sub>3</sub> solution and distilled water and then dried over MgSO<sub>4</sub>. The solvent was removed by rotoevaporation, and the product (compound 1, Figure 1) was further purified by recrystallization from an ethanol–water mixture. Drying under vacuum produced a fine orange powder (0.22 g, 60% yield) with the following characteristics: <sup>1</sup>H NMR

- (15) Xia, Y.; Whitesides, G. M. *Angew. Chem., Int. Ed.* **1998**, *37*, 550.
- (16) Flounders, A. W.; Brandon, D. L.; Bates, A. H. *Biosens. Bioelectron.* **1997**, *12*, 447.
- (17) Mooney, J. F.; Hunt, A. J.; McIntosh, J. R.; Liberko, C. A.; Walba, D. M.; Rogers, C. T. *Proc. Natl. Acad. Sci.* **1996**, *93*, 12287.
- (18) Nicolau, D. V.; Suzuki, H.; Mashiko, S.; Taguchi, T.; Yoshikawa, S. *Biophys. J.* **1999**, *77*, 1126.
- (19) Nicolau, D. V.; Taguchi, T.; Taniguchi, H.; Yoshikawa, S. *Colloids Surf., A* **1999**, *155*, 51.
- (20) Husemann, M.; Morrison, M.; Benoit, D.; Frommer, J.; Mate, C. M.; Hinsberg, W. D.; Hedrick, J. L.; Hawker, C. J. *J. Am. Chem. Soc.* **2000**, *122*, 1844.
- (21) Prucker, O.; Habicht, J.; Park, I.; Ruhe, J. *Mater. Sci. Eng., C* **1999**, *8–9*, 291.
- (22) Ulman, A. *Chem. Rev.* **1996**, *96*, 1533.
- (23) Wallraff, G. M.; Hinsberg, W. D. *Chem. Rev.* **1999**, *99*, 1801.
- (24) Kim, J.; Kang, J.; Han, D.; Lee, C.; Ahn, K. *Chem. Mater.* **1998**, *10*, 2332.
- (25) Aoki, A.; Ghosh, P.; Crooks, R. M. *Langmuir* **1999**, *15*, 7418.
- (26) Crooks, R. M. *ChemPhysChem* **2001**, *2*, 644.
- (27) Dulcey, C. S.; Georger, J. H., Jr.; Chen, M.; McElvany, S. W.; O'Ferrall, C. E.; Benezra, V. I.; Calvert, J. M. *Langmuir* **1996**, *12*, 1638.
- (28) Ingall, M. D. K.; Honeyman, C. H.; Mercure, J. V.; Bianconi, P. A.; Kunz, R. R. *J. Am. Chem. Soc.* **1999**, *121*, 3607.
- (29) Brandow, S. L.; Chen, M.-S.; Aggarwal, R.; Dulcey, C. S.; Calvert, J. M.; Dressick, W. J. *Langmuir* **1999**, *15*, 5429.
- (30) Pease, A. C.; Solas, D.; Sullivan, E. J.; Cronin, M. T.; Holmes, C. P.; Fodor, S. P. A. *Proc. Natl. Acad. Sci. U.S.A.* **1994**, *91*, 5022.

- (29) Frutos, A. G.; Brockman, J. M.; Corn, R. M. *Langmuir* **2000**, *16*, 2192.
- (30) Strother, T.; Knickerbocker, T.; Russell, J. N., Jr.; Butler, J. E.; Smith, L. M.; Hamers, R. J. *Langmuir* **2002**, *18*, 968.
- (31) Prucker, O.; Naumann, C. A.; Ruhe, J.; Knoll, W.; Frank, C. W. *J. Am. Chem. Soc.* **1999**, *121*, 8766.
- (32) Kim, T.; Ye, Q.; Sun, L.; Chan, K. C.; Crooks, R. M. *Langmuir* **1996**, *12*, 6065.
- (33) Kim, T.; Chan, K. C.; Crooks, R. M. *J. Am. Chem. Soc.* **1997**, *119*, 189.
- (34) Huang, J.; Hemminger, J. C. *J. Am. Chem. Soc.* **1993**, *115*, 3342.
- (35) Saminathan, M.; Pillai, C. K. S.; Pavithran, C. *Macromolecules* **1993**, *26*, 7103.
- (36) Prescher, D.; Thiele, T.; Ruhmann, R.; Schulz, G. *J. Fluorine Chem.* **1995**, *74*, 185.
- (37) Stiller, B.; Knochenhauer, G.; Markava, E.; Gustina, D.; Muzikante, I.; Karageorgiev, P.; Brehmer, L. *Mater. Sci. Eng., C* **1999**, *8–9*, 385.
- (38) Wolf, H.; Ringsdorf, H.; Delamarche, E.; Takami, T.; Kang, H.; Michel, B.; Gerber, Ch.; Jaschke, M.; Butt, H.-J.; Bamberg, E. *J. Phys. Chem.* **1995**, *99*, 7102.



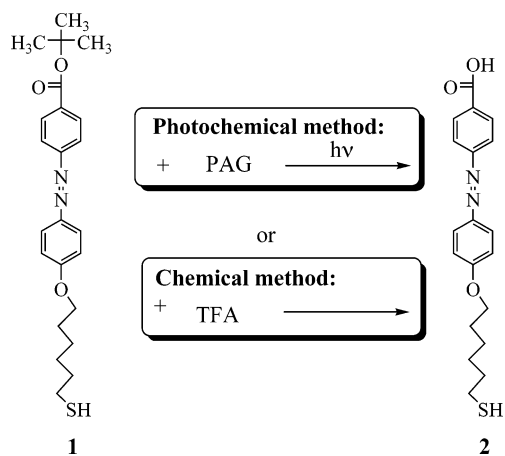


**Figure 1.** A *tert*-butyl ester azobenzene alkanethiol derivative can be either photochemically or hydrolytically converted to a carboxylic acid derivative.

(CDCl<sub>3</sub>)  $\delta$  8.11 (d,  $J$  = 9 Hz, 2H), 7.91 (dd,  $J$  = 9 Hz, 4H), 7.14 (d,  $J$  = 9 Hz, 2H), 4.08 (t,  $J$  = 6 Hz, 2H), 2.48 (m, 2H), 1.85–1.41 (m, 17H), 1.32 (t, 1H). High-resolution mass spectroscopy (HRMS) yielded a mass of 414.1988 compared to the value 414.1628 calculated for C<sub>23</sub>H<sub>30</sub>O<sub>3</sub>N<sub>2</sub>S.

**Compound 2, 4-[4-(6-Mercaptohexyloxy)phenylazo]benzoic Acid.** **2** was obtained by acid-catalyzed deprotection of the *tert*-butyl ester group using trifluoroacetic acid. An excess of trifluoroacetic acid was (99%, Acros) added to 0.2 g of **1**. The mixture was stirred for 5 min to dissolve. The excess trifluoroacetic acid was flushed out by introducing an argon stream to the reaction vessel. Acetone was added to the crude mixture to remove unreacted starting materials. The deprotected product acid was solidified by acetone and filtered out. The solid product (compound **2**, Figure 1) was further purified by washing with several portions of acetone. The yield was 90–95% and the product characteristics were: <sup>1</sup>H NMR (DMSO-*d*<sub>6</sub>)  $\delta$  13.08 (broad, 1H), 8.10 (d,  $J$  = 9 Hz, 2H), 7.89 (dd,  $J$  = 9 Hz, 4H), 7.11 (d,  $J$  = 9 Hz, 2H), 4.06 (t,  $J$  = 6 Hz, 2H), 2.7 (m, 2H), 1.78–1.25 (m, 9H). HRMS ( $M + 1$ ) gave a mass of 359.1441 compared to the theoretical value of 359.1429 for C<sub>19</sub>H<sub>23</sub>O<sub>3</sub>N<sub>2</sub>S.

**Preparation of Azobenzene Alkanethiol SAMs.** SAMs of compound **1** were prepared by immersing gold substrates for 12–24 h in a 1.0–0.1 mM solution of compound **1** in ethanol. The procedure was repeated for compound **2** using tetrahydrofuran. The surfaces were rinsed thoroughly with the corresponding solvent and dried in a stream of nitrogen prior to characterization. The gold substrates were prepared by evaporating 10-nm chromium, followed by 100-nm gold (99.99%), onto 3" N (100) prime grade silicon wafers (Wafer World, Inc.). The silicon wafers were cleaned by "piranha" etching before and after gold deposition, rinsed with copious amounts of deionized water, acetone, and ethanol, and dried in a stream of nitrogen.

**Photochemical Modification and Chemical Patterning.** A sacrificial layer (>1  $\mu$ m) of polystyrene (PS) containing triphenylsulfonium triflate (PAG donated by IBM; 8 wt % PAG/PS) was spin-coated at 2500 rpm/s for 2 min on top of SAM **1** from a (8% w/w) solution of PS/PAG in propylene glycol monomethyl ether acetate (Aldrich). The sample was then exposed to a mercury lamp (254 nm, 760  $\mu$ W/cm<sup>2</sup>) for 10–30 s in the presence of a photomask, which consisted of a metallic disk with spacings of about 280  $\mu$ m. The UV exposed sample was post-baked at 100 °C from 30 s to 1 min to facilitate the diffusion of the photogenerated acid molecules. The remaining excess PAG and PS was removed by washing with toluene.

**Sample Characterization.** UV–vis spectra were obtained using a Shimadzu (UV-2401PC) UV–vis recording spectrophotometer. Contact angle measurements were performed with a Rame-Hart 100-00 contact angle goniometer using Millipore Mili-Q water. A drop of 1- $\mu$ L volume was formed with the use of a micropipet and placed directly onto the sample. At least three droplets were measured on each sample. The sample variation for a given SAM type was less than 2–3°. X-ray photoelectron spectroscopy (XPS) spectra were recorded with a

PHI 5500 model spectrometer equipped with an Al K $\alpha$  monochromator X-ray source run at 15 kV and 23.3 mA, a hemispherical electron energy analyzer, and a multichannel detector. The test chamber pressure was maintained below  $2 \times 10^{-9}$  Torr during spectral acquisition. A low-energy electron flood gun was used to neutralize the possible surface charge. The XPS binding energy (BE) was internally referenced to the aliphatic C(1s) peak (BE = 284.6 eV). Survey spectra were acquired at an analyzer pass energy of 93.9 eV and BE resolution of 0.8 eV, while high-resolution spectra were acquired with a pass energy of 23.5 eV and BE resolution of 0.05 eV. The takeoff angle is defined as the angle between the surface normal and detector. Angle-dependent XPS (ADXPS) was performed by using a motor to rotate the sample holder to the desired takeoff angle. High-resolution spectra were resolved by fitting each peak with Gaussian–Lorentz functions after subtracting the background using the PHI data processing software package under the constraint of setting a reasonable BE shift and characteristic full width at half-maximum range. Atomic concentrations were calculated by normalizing peak areas to the elemental sensitivity factor data provided by the PHI database.

Fluorescence imaging of surfaces was performed using an Olympus IX70 laser scanning confocal microscope equipped with an Ar laser as an excitation source. The sample was excited at 488 nm, and the corresponding emission was collected above 510 nm. Fluorescence intensity was monitored as a function of *X–Y* position as the sample was focused above the laser beam through a 20 $\times$  or 10 $\times$  objective. Fluorescence images (512  $\times$  512 pixels) were typically acquired at a photomultiplier tube voltage of 900 V and a scan speed of 16 scans/s. Light micrographs were recorded using a Nikon Optiphot metallurgical dark field microscope equipped with a Kodak MDS digital camera in the reflection mode. The image was typically acquired using 20 $\times$  and 5 $\times$  objectives.

**Visualization of the Chemically Patterned Surface.** Chemical surface patterns were visualized by three methods: by condensing water onto the patterned surface,<sup>39,40</sup> by non-covalent interaction mediated adsorption of amine-functional PS colloidal particles (diameter 3  $\mu$ m, 2.6% solid latex suspension; PolyScience, Inc.), and by decoration with fluorescein-tagged PS nanoparticles (diameter 57 nm; PolyScience, Inc.). Particle assembly was performed either through the controlled evaporation of solvent or particle-surface adsorption in an aqueous medium. Patterning by controlled evaporation was achieved by applying a drop of diluted solid latex suspension (0.1% w/w) containing PS colloidal particles on top of the patterned azobenzene SAM samples. The samples were slightly heated at 50 °C from 1 to 3 h until the water evaporated completely. Patterning by adsorption was achieved by "dip-coating". Patterned substrates were immersed completely in a latex suspension with 0.1% solid content and incubated overnight. The substrates were then removed, washed with water, and dried under a stream of N<sub>2</sub>.

## Results and Discussion

The basis of our method for light-induced surface modification and direct chemical-group surface patterning is the molecular design and synthesis of a difunctional azo compound, compound **1**, as illustrated in Figure 1. The *tert*-butyl ester functionality provides a site for a photochemical change from a hydrophobic *tert*-butyl group to a reactive hydrophilic carboxylic acid group. This same photochemical change forms the basis of chemical amplification photoresist technology.<sup>41</sup> When exposed to UV light, the PAG produces a proton that catalyzes the deprotection of the *tert*-butyl ester (compound **1**, SAM **1**) to form a carboxylic acid (compound **2**, SAM **2**) and butylene gas. Photodeprotection of the hydrophobic *tert*-butyl ester to form a carboxylic acid offers a photochemical alternative to more traditional chemical deprotection

(39) Lopez, G. P.; Biebuyck, H. A.; Frisbie, C. D.; Whitesides, G. M. *Science* **1993**, 260, 647.

(40) Kumar, A.; Whitesides, G. M. *Science* **1994**, 263, 60.

(41) Paul, R.; Schmidt, R.; Dyer, D. J. *Langmuir* **2002**, 18, 8719.

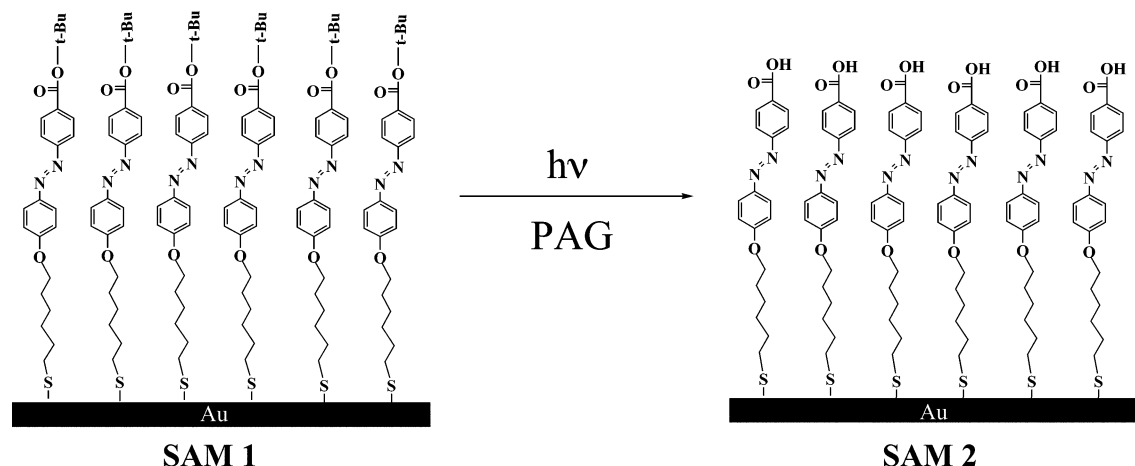


**Figure 2.** A SAM of compound **1** with a *tert*-butyl ester surface functionality is photochemically converted to a SAM of compound **2** with a carboxylic acid surface functionality by exposure to deep UV radiation in the presence of a PAG.

methods, such as hydrolysis with trifluoroacetic acid,<sup>42</sup> also described in Figure 1. Both of these deprotection schemes occur readily in solution to produce an acid-terminated azobenzene alkanethiol compound.

The photochemical transformation reaction of Figure 1 can be used to modify surface properties if it can be confined to a surface. For this purpose, the azo compound is functionalized at its other terminus with an alkanethiol group to promote self-assembly at the surface of coinage metals such as gold. Self-assembly of SAM **1** causes the *tert*-butyl ester group to locate at the SAM–air interface, as depicted in Figure 2. A layer of PAG is then applied onto the SAM-coated gold substrate by spin coating (using PS as a carrier). Exposure to UV light and subsequent stripping of the surface PAG-containing overlayer converts the initially hydrophobic surface covered with *tert*-butyl groups to a hydrophilic surface covered with reactive carboxylic acid groups.

The SAMs represented in Figure 2 were characterized by water contact angle measurements and XPS. The measured water contact angles were  $89 \pm 2^\circ$  for SAM **1** and  $28 \pm 3^\circ$  for SAM **2**, confirming the expected change in hydrophilicity from hydrophobic *tert*-butyl end groups to hydrophilic carboxylic acid end groups.

The XPS spectra shown in Figure 3 provide quantitative confirmation of the photochemical surface modification reaction depicted in Figure 2. The high-resolution C(1s) spectra for both the *tert*-butyl ester and photodeprotected carboxylic acid surfaces show evidence of four different types of carbon. The signal at 284.6 eV is associated with aliphatic and aromatic carbons that are not bonded to oxygen, the 285.7 eV signal is associated with carbons in ether linkages, the 286.8 eV signal is associated with the ester carbon in the *tert*-butyl group, and the 288.7 eV signal is associated with the carbonyl ester carbon. The large loss of the signal at 286.8 eV (see Figure 3a) confirms almost complete removal of the *tert*-butyl group after photodeprotection.

XPS can also be employed to confirm that the functional monolayers are oriented normal to the surface, as pictured in Figure 2 through analysis of the integrated peak intensities associated with each carbon type. The C(1s) peaks at 288.7, 286.8, 285.7, and 284.6 eV have intensity ratios of 1:1:3:14 for SAM **1** (a) and 1:2:3:17 for SAM **2** (b). These values cannot, however, be interpreted directly because XPS is an integral technique. The signal for a

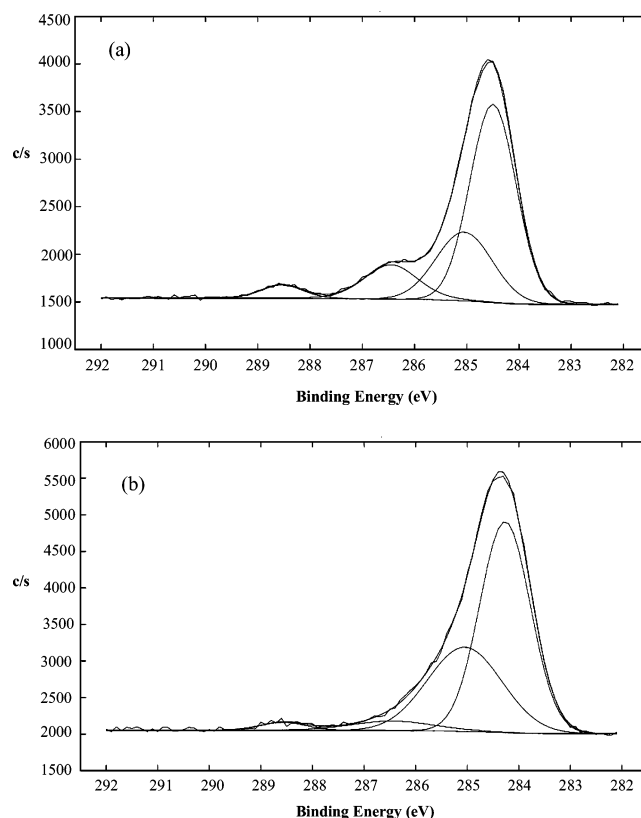


**Figure 3.** High-resolution C(1s) XPS spectra of SAM **1** (a) and SAM **2** (b).

particular spectral peak is related to the integral of the composition depth profile of the associated carbon atom weighted by the probability of escape for the corresponding ejected photoelectron. This relationship is given by<sup>43</sup>

$$I_i(\theta) = K_i \int_0^\infty N_i(x) e^{-x/\lambda \sin \theta} dx \quad (1)$$

where  $\theta$  is the photoelectron takeoff angle,  $K_i$  is a constant for carbon type  $i$ ,  $\lambda$  is the photoelectron mean free path, and  $N_i(x)$  is the composition depth profile of carbon type  $i$ . Knowledge of the composition depth profile,  $N_i(x)$ , is, therefore, necessary to correctly calculate the ratios of different carbon signals. The atomic distribution functions,

(42) Ma, Q.; Wooley, K. L. *J. Polym. Sci., Part A: Polym. Chem.* **2000**, *38*, 4805.

(43) Andrade, J. D. *Surface and Interfacial Aspects of Biomedical Polymers*; Plenum Press: New York, 1985; Vol. 1, Chapter 5.

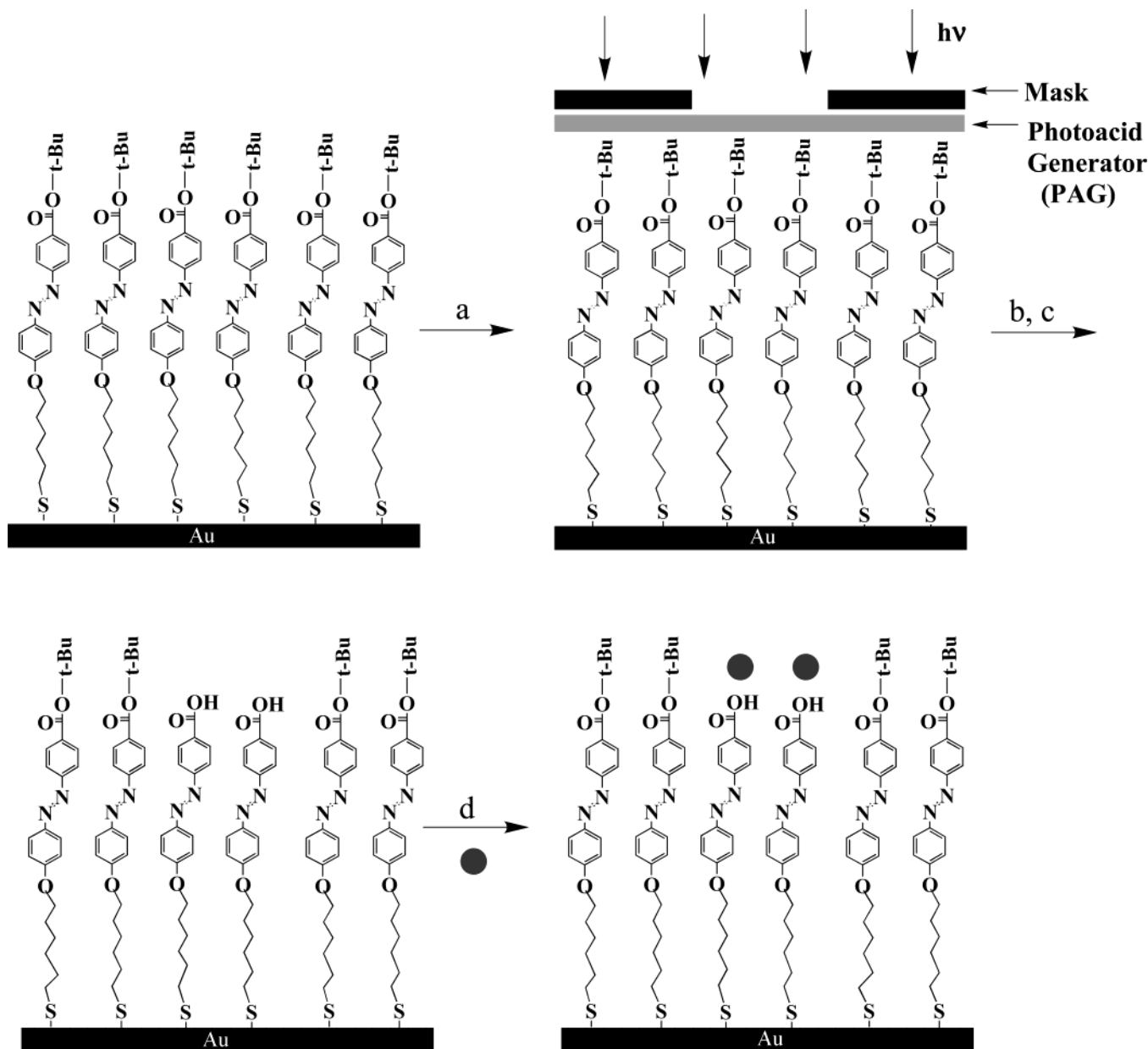


**Figure 4.** Strategy for direct chemical patterning of a SAM surface using a photolithographic technique: (a) Spin-coat PAG and cover with a photomask, (b) irradiate, (c) post-bake and remove soluble PAG, and (d) decorate the surface with ligands (filled circles).

$N_i(x)$ , were estimated by applying Chem3D to model the SAMs in an all-trans extended conformation oriented perpendicular to the substrate. Once the positions of each atom were calculated, eq 1 was applied to calculate the XPS signals of each individual carbon in the SAMs. The total carbon, nitrogen, and oxygen signals calculated in this fashion and summed over all the atoms are reported in Table 1, where they are compared to experimentally determined atomic percentages. The nitrogen signals do not compare well, however, because these are weak signals due to the low intrinsic photoelectron yield for nitrogen and are subject to large errors. The carbon and oxygen signals predicted by the molecular model assuming normal orientation agree well with the experimental values, supporting the hypothesis that molecules within the SAMs are oriented normal to the substrate.

The thickness of the monolayers may be estimated through ADXPS measurements wherein the photoelectron takeoff angle is systematically varied. The thickness of the SAMs was evaluated by measuring the ratio of signals originating in the overlayer [C(1s)] and the substrate

**Table 1.** XPS Determination of Elemental Compositions at a 45° Take-Off Angle and ADXPS Estimated Thicknesses ( $t$ ) of SAM 1 and SAM 2

	C (%)	O (%)	N (%)	$t$ (nm)
<b>SAM 1</b>				
theory <sup>a</sup>	81.9	11.5	6.64	2.16
experiment <sup>b,c</sup>	82.8	12.6	2.2	2.13
<b>SAM 2</b>				
theory <sup>a</sup>	77.0	14.7	8.31	2.16
experiment <sup>b,c</sup>	79.3	15.7	3.6	2.10

<sup>a</sup> The theoretical value of the elemental composition is calculated from the molecular structure. <sup>b</sup> The uncertainty of the abundant elements C and O is  $\pm 5\%$ . <sup>c</sup> The uncertainty of the trace element N is  $\pm 15\%$ .

[Au(4f<sub>7/2</sub>)] as a function of the takeoff angle and regressing these data to the uniform overlayer model.<sup>41,44,45</sup> The XPS-estimated thickness values agree well with values for

(44) Fadley, C. S. *Prog. Solid State Chem.* **1976**, *11*, 265.

(45) Ulman, A. *Characterization of Organic Thin Films*; Butterworth-Heinemann, Inc.: Boston, 1985; p 221.



similar azobenzene SAMs measured by X-ray reflectivity and ellipsometry and are comparable to the theoretical thickness (see Table 1),  $2.16 \pm 0.30$  nm, obtained by modeling the molecular structure from known bond lengths.<sup>46–48</sup> The thickness data indicate that the azobenzene SAMs possess a molecular orientation that is essentially normal to the substrate, consistent with the high packing density, molecular order, and stability provided by  $\pi$ – $\pi$  interactions of the azobenzene units. An orientation slightly tilted from the normal orientation was previously found for other aromatic thiol monolayers on Au(111).<sup>49–54</sup> In this case, the molecular orientation was deduced from a comparison of experimental and theoretical thickness data.

The XPS and contact angle analyses confirm that *tert*-butyl-terminated azobenzene alkanethiols self-assemble onto gold substrates in a nearly normal orientation and that the surface of these SAMs can be converted from hydrophobic *tert*-butyl groups to hydrophilic carboxylic acid groups by exposure to UV light in the presence of a PAG. Self-assembling monolayers with functional termini that can be photodeprotected by exposure to UV light, therefore, constitute an exciting new method for modifying surface chemical structure and properties at the molecular level.

A second objective of this paper is to demonstrate that photochemical surface modification can also be adapted to chemically patterned surfaces. Figure 4 shows how the surface of SAM 1 can be photochemically modified to deliberately create a heterogeneous pattern of hydrophobic and hydrophilic regions. End-functional azobenzene alkanethiols are first self-assembled onto a gold substrate and then coated with a layer of PAG supported in PS by spin coating. The surface is subsequently covered with a patterned photomask and irradiated with UV light. Unmasked regions on the surface are photodeprotected to form carboxylic acid-terminated regions, while unexposed regions retain *tert*-butyl functionality. The resulting heterogeneous surface serves as a template for the subsequent deposition of a variety of objects and ligands into patterns with microscale resolution.

Surface patterns generated by the photochemical surface modification technique cannot usually be observed by the eye because the modifications involved generally do not produce large changes in the thickness or refractive index. Surface patterns can be observed, however, using a variety of visualization techniques. Figure 5 compares images of the hydrophobic SAM 1 surface (a), the hydrophilic SAM 2 surface (b), and the patterned SAM surface (c) visualized by exposure to water vapor. In part a,

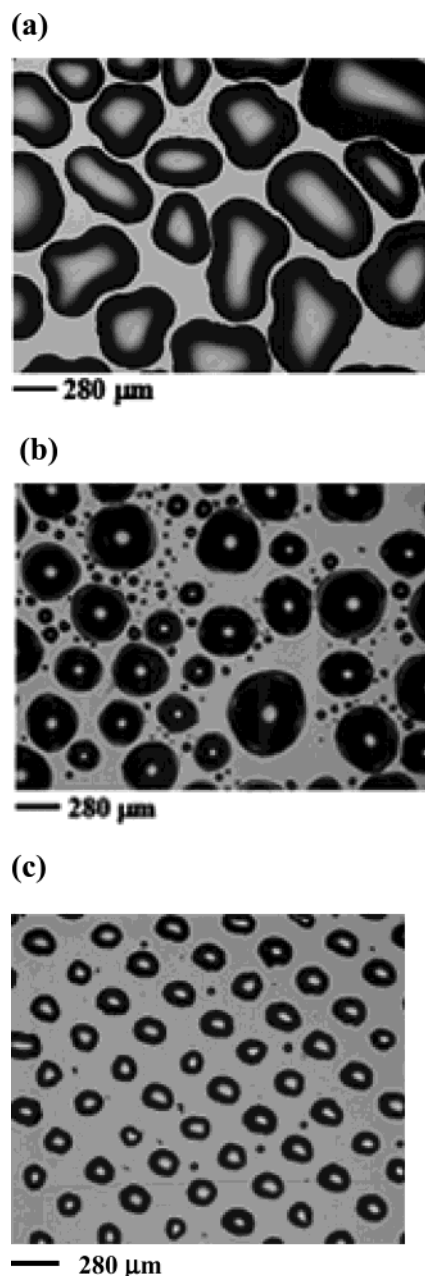


**Figure 5.** Optical microscope images of water condensation on the SAM surfaces: (a) SAM 1 (*tert*-butyl-terminated azobenzene alkanethiol), (b) SAM 2 (COOH-terminated azobenzene alkanethiol), and (c) patterned surface. The surface was patterned by UV exposure through a 280- $\mu$ m grid.

macroscopic water droplets condense and bead up on the hydrophobic *tert*-butyl ester-terminated monolayer surface (shown previously to have a water contact angle of 89°). In part b, the water droplets are again macroscopic but partially wet the substrate (with a contact angle of 28°). In part c, a well-ordered microscale array of water droplets is observed as water vapor preferentially condenses onto the more hydrophilic carboxylic acid functional sites produced by exposure through the mask. The masked *tert*-butyl ester-terminated regions act as hydrophobic dams that restrict water to spread only onto the photodeprotected carboxylic acid regions. As a control experiment, SAM 1 was irradiated in the absence of the PAG. A pattern was not observed, indicating that the *tert*-butyl group is only photolabile in the presence of PAG.

Photochemically patterned surfaces may also be visualized by using them to template the adsorption of a variety

(46) Siewierski, L. M.; Brittain, W. J.; Petrash, S.; Foster, M. D. *Langmuir* **1996**, *12*, 5838.

(47) C–C = 1.545 Å, C–S = 1.81 Å, C–H = 1.1 Å, C–O = 1.36 Å, Au–S = 1.5 Å, C–C (in benzene ring) = 1.399 Å, C–N (in azobenzene) = 1.247 Å, C–O (in –COOH) = 1.364 Å, O–H = 1 Å. All values are taken from *Handbook of Chemistry and Physics*, 3rd electronic ed.; CRC Press: Boca Raton, FL.

(48) Han, S. W.; Kim, C. H.; Hong, S. H.; Chung, Y. K.; Kim, K. *Langmuir* **1999**, *15*, 1579.

(49) Tour, J. M.; Jones, L. II; Pearson, D. L.; Lamba, J. S.; Burgin, T. P.; Whitesides, G. M.; Allara, D. L.; Parikh, A. N.; Atre, S. V. *J. Am. Chem. Soc.* **1995**, *117*, 9529.

(50) Sabatani, E.; Cohen-Boulakia, J.; Bruening, M.; Rubinstein, I. *Langmuir* **1993**, *9*, 2974.

(51) Tao, Y. T.; Wu, C. C.; Eu, J. Y.; Lin, W. L. *Langmuir* **1997**, *13*, 4018.

(52) Dhirani, A.-A.; Zehner, R. W.; Hsung, R. P.; Guyot-Sionnest, P.; Sita, L. R. *J. Am. Chem. Soc.*

(53) Frey, S.; Stadler, V.; Heister, K.; Eck, W.; Zharnikov, M.; Grunze, M.; Zeysing, B.; Terfort, A. *Langmuir* **2001**, *17*, 2408.

(54) Ishida, T.; Choi, N.; Mizutani, W.; Tokumoto, H.; Kojima, I.; Azebara, H.; Hokari, H.; Akiba, U.; Fujihira, M. *Langmuir* **1999**, *15*, 6799.

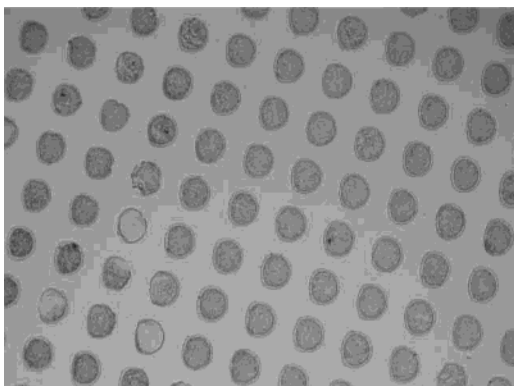


**Figure 6.** Optical microscope image of PS-NH<sub>2</sub> (3 μm) particles adsorbed onto a chemically photopatterned surface. The surface was patterned by UV exposure through a 280-μm grid.

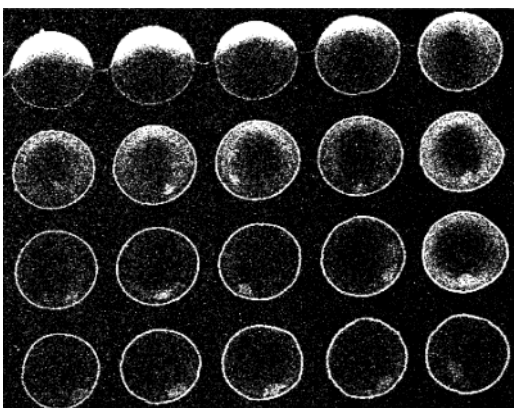


**Figure 7.** Fluorescent confocal microscope image of a photochemically patterned surface after decoration with fluorescein-tagged PS nanoparticles (57 nm).

of ligands. Because of the amphiphilic nature of chemically patterned surfaces, it is possible to template ligands through either hydrophobic interactions with *tert*-butyl functionality or hydrophilic interactions with the carboxylic acid functionality. A suspension of amine-functionalized PS (PS-NH<sub>2</sub>) colloidal particles (3-μm diameter) in an aqueous solution, for example, was prepared and deposited on a surface patterned with a 280-μm grid. The optical microscope image shown in Figure 6 demonstrates that the PS-NH<sub>2</sub> colloidal particles selectively adsorb onto UV-exposed regions patterned with surface carboxylic acid groups by nature of noncovalent interactions.

Materials on the nanoscale can also ligate to the photochemically patterned surface. Amine-terminated fluorescein-labeled PS nanoparticles (57 nm) were tested for this purpose. Figure 7 shows a fluorescent confocal microscope image of the decorated surface, confirming that the nanoparticles deposited selectively on carboxylic acid regions on the surface. Photochemically patterned surfaces, therefore, serve as effective means for templating two-dimensional geometric patterns of a variety of objects and molecules.

### Summary

A new photolithographic technique for direct photochemical modification and chemical patterning of surfaces is described. The technique involves the self-assembly of *tert*-butyl ester end-functional alkanethiols onto gold substrates. XPS experiments confirm that (1) self-assembly causes terminal *tert*-butyl ester groups to locate at the air-monolayer interface and (2) the *tert*-butyl ester groups are subsequently converted to carboxylic acid groups when exposed to UV radiation in the presence of a PAG. The photochemical change from hydrophobic *tert*-butyl ester groups to hydrophilic groups has a profound effect on surface wettability, as reflected in a water contact angle change from 89 to 28°. Surfaces may be patterned with this process on a microscale by exposure to UV light through a patterned photomask. Unexposed regions retain the properties associated with hydrophobic *tert*-butyl ester end groups, while exposed regions are converted to a carboxylic acid surface chemical functionality. Finally, we demonstrate that the photomasking technique is an effective and simple means for templating two-dimensional surface deposition of a variety of molecules and objects. The resultant hydrophobic and hydrophilic surface regions can be used to spatially pattern fluid wetting (i.e., water), the adsorption of amine-terminated PS colloidal particles, and the deposition of amine-terminated, fluorescein-labeled PS nanoparticles. The surface patterning technique retains the full resolution of deep UV photolithography, requires only light and a PAG as reagents, and can be performed with conventional deep UV photomasking systems.

**Acknowledgment.** This material is based upon work supported by, or in part by, the U.S. Army Research Office under Contract/Grant DAAD19-06-1-0104 and in part by the MRSEC Program of the National Science Foundation under Award No. DMR-02-13574.

LA0358163